DOE/MC/31160 -- 5117
(DE96004345)

Particulate Hot Gas Stream Cleanup Technical Issues
Task 1.0 -- Assessment of Ash Characteristics

Quarterly Report
October - December 1994

March 1995

Work Performed Under Contract No.: DE-AC21-94MC31160

For
U.S. Department of Energy
Office of Fossil Energy
Morgantown Energy Technology Center
Morgantown, West Virginia

By
Southern Research Institute
Birmingham, Alabama

DISCLAIMER

PARTICULATE HOT GAS STREAM CLEANUP TECHNICAL ISSUES TASK 1.0 – ASSESSMENT OF ASH CHARACTERISTICS

DOE/MC/31160 -- 5117
(DE96004345)
Distribution Category UC-106

Particulate Hot Gas Stream Cleanup Technical Issues Task 1.0 -- Assessment of Ash Characteristics

Quarterly Report October - December 1994

Work Performed Under Contract No.: DE-AC21-94MC31160

For
U.S. Department of Energy
Office of Fossil Energy
Morgantown Energy Technology Center
P.O. Box 880
Morgantown, West Virginia 26507-0880

By
Southern Research Institute
2000 Ninth Avenue South
P.O. Box 55305
Birmingham, Alabama 35255-5305

March 1995

TABLE OF CONTENTS

INTRODUCTION

This is the first in a series of quarterly reports describing the activities performed under Task 1 of Contract No. DE-AC21-94MC31160. The analyses of Hot Gas Stream Cleanup (HGCU) ashes and descriptions of filter performance presented in this report were designed to address the problems with filter operation that are apparently linked to the characteristics of the collected ash. These problems include excessive filtering pressure drop, the formation of large, tenacious ash deposits within the filter vessel, and bent or broken candle filter elements. Characterization of new and used filter elements will be performed under Task 2 of this contract. Much of the work planned for Task 1 builds directly on work performed under a prior contract (No. DE-AC21-89MC26239).

OBJECTIVES

This task has two primary objectives. The first is to generate a readily accessible data base of the key characteristics of ashes collected from operating advanced particle filters. The second objective is to relate these ash properties and the contents of the data base to the operation and performance of the advanced particle filters and filter components. The first objective includes formatting the data base, and collecting, analyzing, and maintaining ashes from operating HGCU facilities. The second objective involves the collection of operating histories from advanced particle filters, correlating these histories with ash characteristics, interpreting these correlations, and communicating our conclusions in the various venues prescribed by the U.S. Department of Energy's Morgantown Energy Technology Center (DOE/METC).

BACKGROUND

A significant amount of work that was performed under Contract No. DE-AC21-89MC26239 will be utilized to meet the stated objectives of this task. Approximately 150 ash samples that have been collected or received from eight HGCU sources have been catalogued and stored. Many of these samples have been subjected to a variety of laboratory analyses. Two visits to the 70 MWe Pressurized Fluidized-Bed Combustion (PFBC) Facility at the Tidd Plant were made during this prior contract to collect samples and observe and record the condition of the Advanced Particulate Filter (APF). Observations of the filter assembly during these visits and laboratory analyses of ashes and ash deposits collected from the APF demonstrated that the ash deposits that form in the APF apparently induce bent and/or broken ceramic candle filter elements.

Two topical reports covering the collection and analyses of HGCU ashes were also issued under Contract No. DE-AC21-89MC26239. The first report, *Assessment of Ash Characteristics from Gas Stream Cleanup Facilities*, covered samples obtained and analyzed between October 1992 and September 1993. The second report, *Updated*

EXECUTIVE SUMMARY

This is the first in a series of quarterly reports describing the activities performed under Task 1 of Contract No. DE-AC21-94MC31160. The analyses of Hot Gas Stream Cleanup (HGCU) ashes and descriptions of filter performance presented in this report were designed to address the problems with filter operation that are apparently linked to the characteristics of the collected ash. This task is designed to generate a data base of the key characteristics of ashes collected from operating advanced particle filters (APF's) and to relate these ash properties to the operation and performance of these filters and their components.

Observations of the filter assembly during site visits to the Tidd Demonstration Plant APF have led to the conclusion that that tenacious ash deposits that form in the APF apparently induce stresses that result in bent and/or broken ceramic candle filter elements. A site visit was made to the Tidd APF on October 27, 1994 to collect ash samples from various locations in the filter vessel and to document the condition of the APF. Although the condition of the APF was somewhat better than during past inspections, a significant number of broken filter elements were observed. Even though the Tidd APF has recently been operating with 25 % of the filter elements removed to reduce ash bridging, several large ash bridges between filter elements and the plenum support columns and/or the ash shedding cones were present when the APF was opened.

A variety of laboratory analyses were performed on ash samples collected during this site visit to assess whether recent attempts to introduce larger particles into the ash deposits by derating the cyclone upstream of the APF have been successful. Some particles larger than 45 μm were identified in various ash samples from the APF, but they account for less than 5 % of the mass of the ash.

Although Scanning Electron Microscope EDX spectra and elemental maps lack the resolution to identify the bonds between particles in the ash agglomerates found in the APF, an excellent stereographic image of the structure of an ash nodule collected from the APF was generated with the Scanning Electron Microscope. The stereographic image was very enlightening as to the structure of the nodule. The nodule appears to be a concretion composed of discrete fine particles almost completely embedded in a pervasive amorphous mass which apparently formed in the APF after the particles were initially collected.

Plans for the next quarter include additional analyses to further quantify the distribution of relatively large particles over the various ash deposits obtained from the Tidd APF. Chemical analyses may also be used to identify the composition, and possibly the mechanism of formation, of the concretion mentioned above.

Assessment of Ash Characteristics from Gas Stream Cleanup Facilities, is still in draft form, and covers samples obtained and analyzed between October 1993 and August 1994. Because operating experiences with HGCU facilities continue to accumulate, this task will continue many of the same types of analyses described in these two topical reports.

RESEARCH ACTIVITIES DURING THE REPORTING PERIOD

OPERATION AND PERFORMANCE OF THE TIDD APF

Recent operation of the APF at the Tidd Demonstration Plant has focused on two separate approaches to eliminating the ash bridges that have formed between candle filter elements and nearby surfaces. The first approach involved increasing the mean size of the entrained particles entering the filter vessel by derating the cyclone located just upstream of the filter. The other approach was to remove the inner ring of candle filter elements from the top two plenum assemblies. Although this latter approach involved removing 25 % of the ceramic candle filter elements, and consequently 25 % of the active surface area, it was implemented to increase the separation between the candle filter elements and the ash shedding cones, reducing the likelihood that ash bridges would form at this location.

Figure 1 shows the general configuration of the APF at Tidd. When the APF was opened on October 27, 1994, we examined the condition of the filter and collected a suite of ash samples from various locations in the APF for analysis. A significant number of candle filter elements were broken, and ash deposits were present at various locations throughout the filter assembly. As we had observed in two previous site visits, the region under each tube sheet where the candle filter elements are mounted to the tube sheet was completely packed with ash deposits. Although the number of ash bridges adjacent to the filter elements was reduced compared to what we saw in our two prior observations, there were still a few large ash bridges formed between the lower portion of filter elements in the top two plenums and the ash shedding cones and/or the plenum support columns. In general, the filtering surfaces of the intact filter elements were relatively clean, except for regions of the candles just below the tube sheet deposits mentioned above. The surfaces of the plenum support columns and the ash shedding cones were cleaner than we had observed previously; however, several thick ash deposits were present on portions of these surfaces. Bridging of ash between filter elements in the bottom plenum did not seem to be a serious problem.

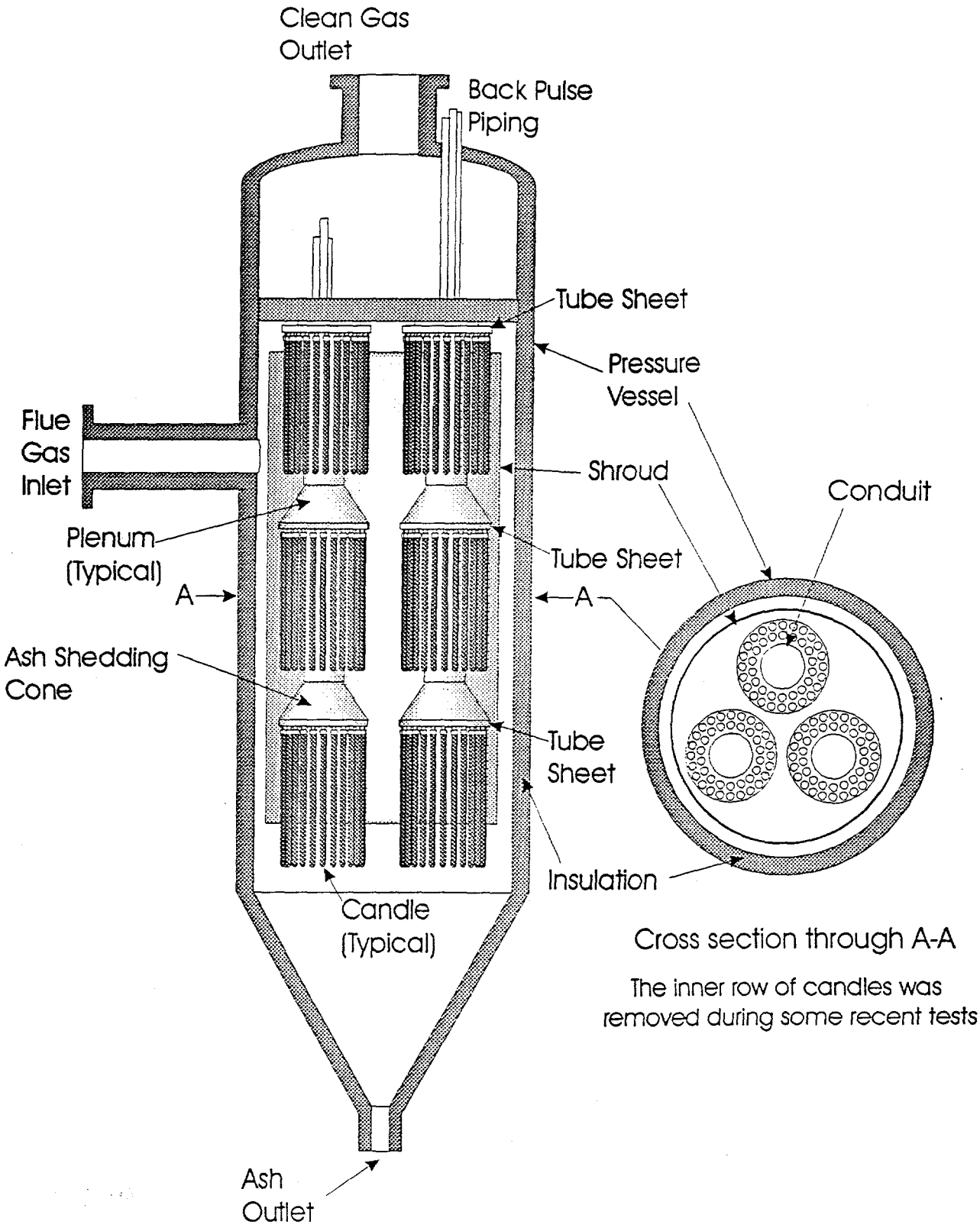

Figure 1. General features of the advanced HGCU system at the Tidd Demonstration Plant.

COLLECTION OF SAMPLES

Table 1. Ash Samples Collected at Tidd on October 27, 1994

ID #	Location	Description/Comments
4096	MP, PSC	
4097	BP, TS	with agglomerates
4098	FC from midway up BP	
4099	FC from lowest 6 inches of BP	
4100	ash from inner wall of pressure vessel	
4101	BP, AB	with agglomerates
4102	BP, FC from inner candles	
4103	BP, FC from third ring of candles (near center of plenum)	
4104	TP, PSC/AS	deposit near junction of PSC and AS (with agglomerates)
4105	TP, AS	with agglomerates (deposit about 1 inch thick)
4106	TP, PSC	thin deposit halfway up PSC
4107	TP, TS	some color variation
4108	TP, TS	light brown ash from 4107
4109	MP, from inside of candle B-8	
4110	TP, FC from outer surface of candle	
4111	MP, FC	
4112	TP, FC from inner surface of candle	
4113	MP, AB	with agglomerates
4114	MP, AS	large agglomerates
4115	TP, AB	large agglomerates
4116	MP, AB	large agglomerates
4117	APF outlet tube	deposited inside outlet tube

AB = Ash Bridge between Candles
APF = Advanced Particulate Filter
AS = Ash Shedding Cone
BP = Bottom Plenum
PSC = Plenum Support Column/Conduit
FC = Filter Cake Ash from Candle Surface
MP = Middle Plenum
TP = Top Plenum
TS = Underside of Tube sheet

ANALYSIS OF SAMPLES

At the request of DOE/METC, we sent a portion of all the ash samples we collected to Dr. T.K. Chiang at DOE/METC and Dr. John Hurley at the University of North Dakota's Energy and Environmental Research Center. (There was not enough of sample ID # 4117 [APF outlet tube] to split. Therefore Southern Research Institute has retained all of this particular sample.) Depending on the type of ash sample being analyzed, and on the specific question(s) under investigation, we select appropriate tests from a suite of laboratory analyses. Appendix A provides brief descriptions of key analyses that we have previously used to characterize HGCU ashes.

In order to compare the characteristics of these ashes with the characteristics of ashes we obtained in September 1993 and May 1994 under Contract No. De-AC21-89MC26239, we also performed limited analyses on the three samples listed in Table 2.

Table 2
Samples Previously Obtained from Tidd used for Comparison with October 1994 Samples

ID #	Date Obtained	Location in Filter Vessel
2998	9/30/93	MP, AS
4079	5/5/94	MP, FC
4084	5/5/94	TP, AS

Measurements of Size Distribution

To identify the extent to which relatively large particles become included in the ash deposits in the filter vessel, we performed sedigraphic analyses of several of the samples we obtained. In each case, the ash size distribution is distinctly bimodal. However, the relative scarcity of large particles in these samples does not allow the sedigraph to yield a reliable determination of the size distribution above about 20 μm. (To introduce more large particles into the measuring cell for analysis, an excessive amount of fine particles would be included also. The sedigraphic analysis cannot be performed if the concentration of the suspension is too high.) The size distributions we measured are presented in Figures 2 through 10. (Figures 2 through 9 present only the finer portion of the size distribution of these ashes. A complete size distribution of one of the ashes is presented in Figure 10.) The mass mean diameters (MMD's) of these distributions are presented in Table 3.

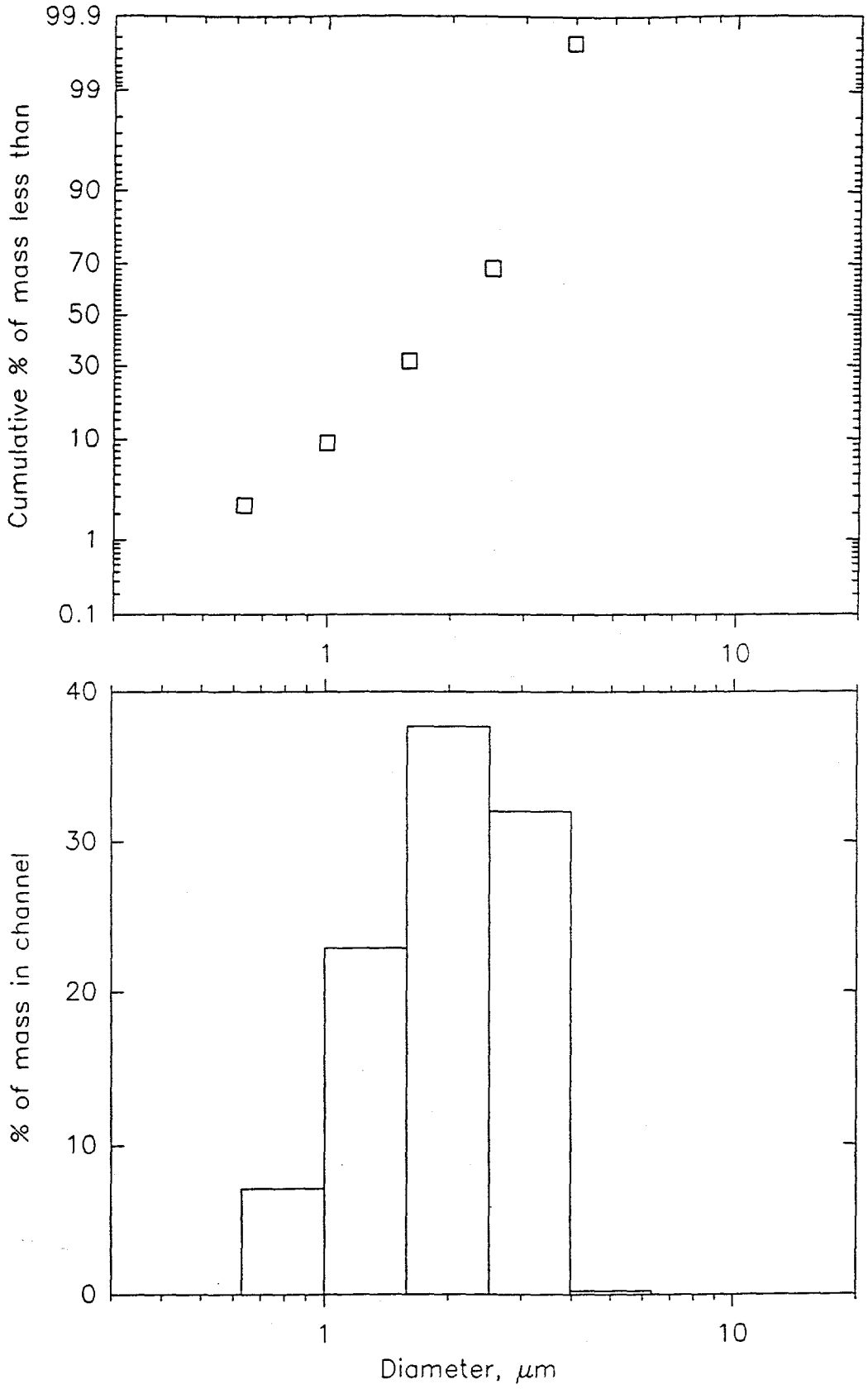

Figure 2. Cumulative and differential size distribution data measured with the sedigraph for ID # 2998 (MP, AS). The MMD of this ash is 2.0 μm.

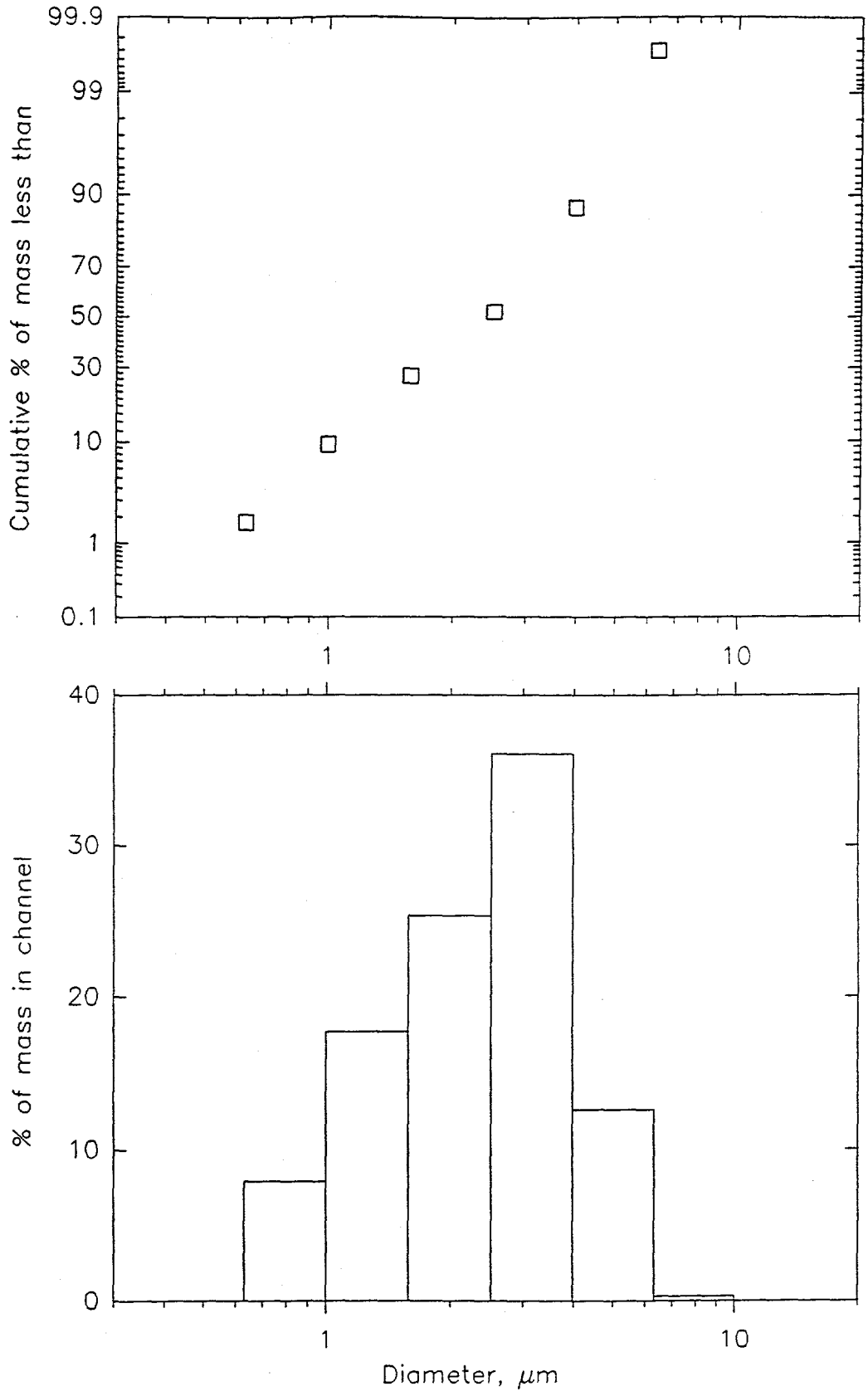

Figure 3. Cumulative and differential size distribution data measured with the sedigraph for ID # 4079 (MP, FC). The MMD of this ash is 2.4 μm.

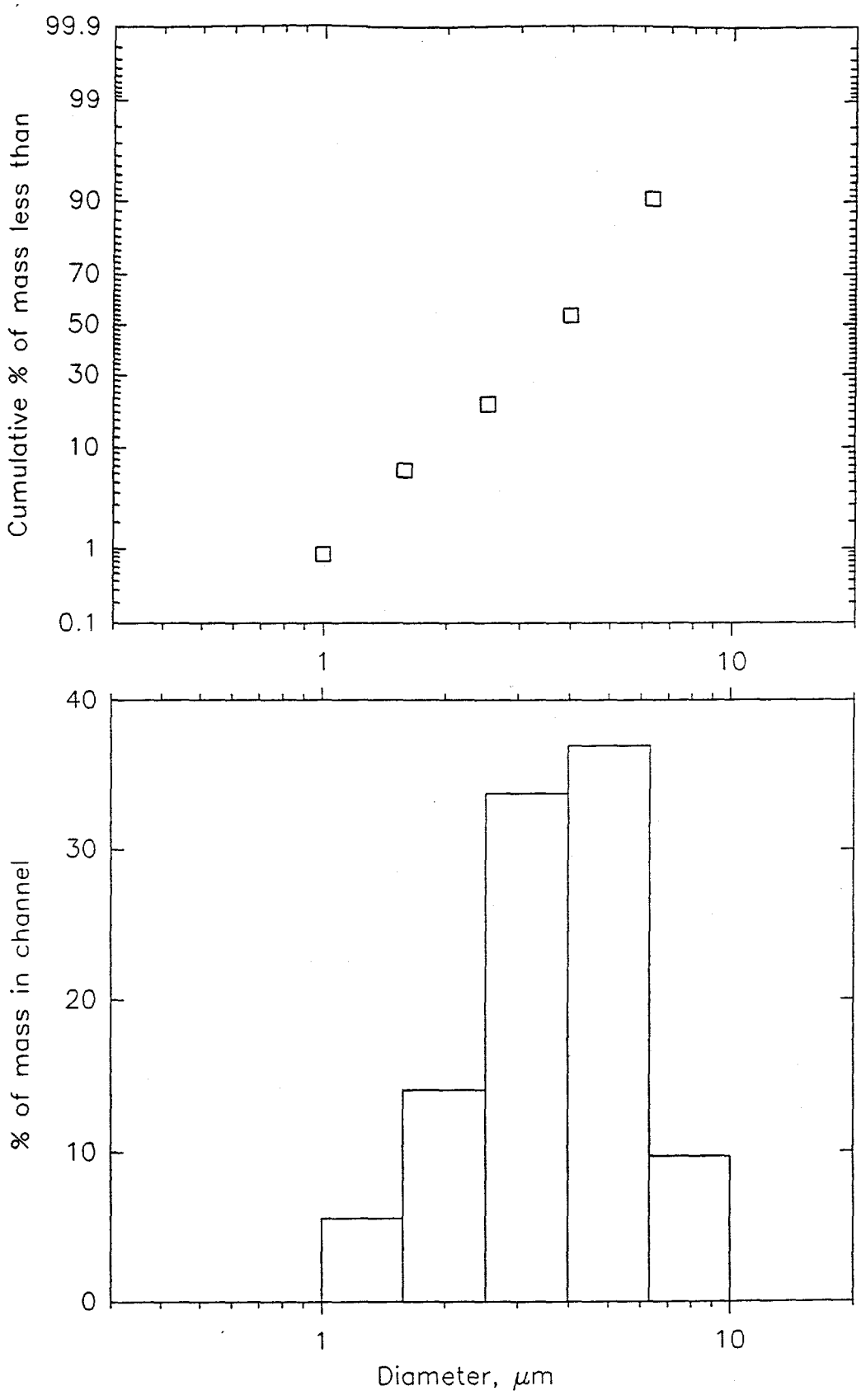

Figure 4. Cumulative and differential size distribution data measured with the sedigraph for ID # 4084 (TP, AS). The MMD of this ash is 3.8 μm.

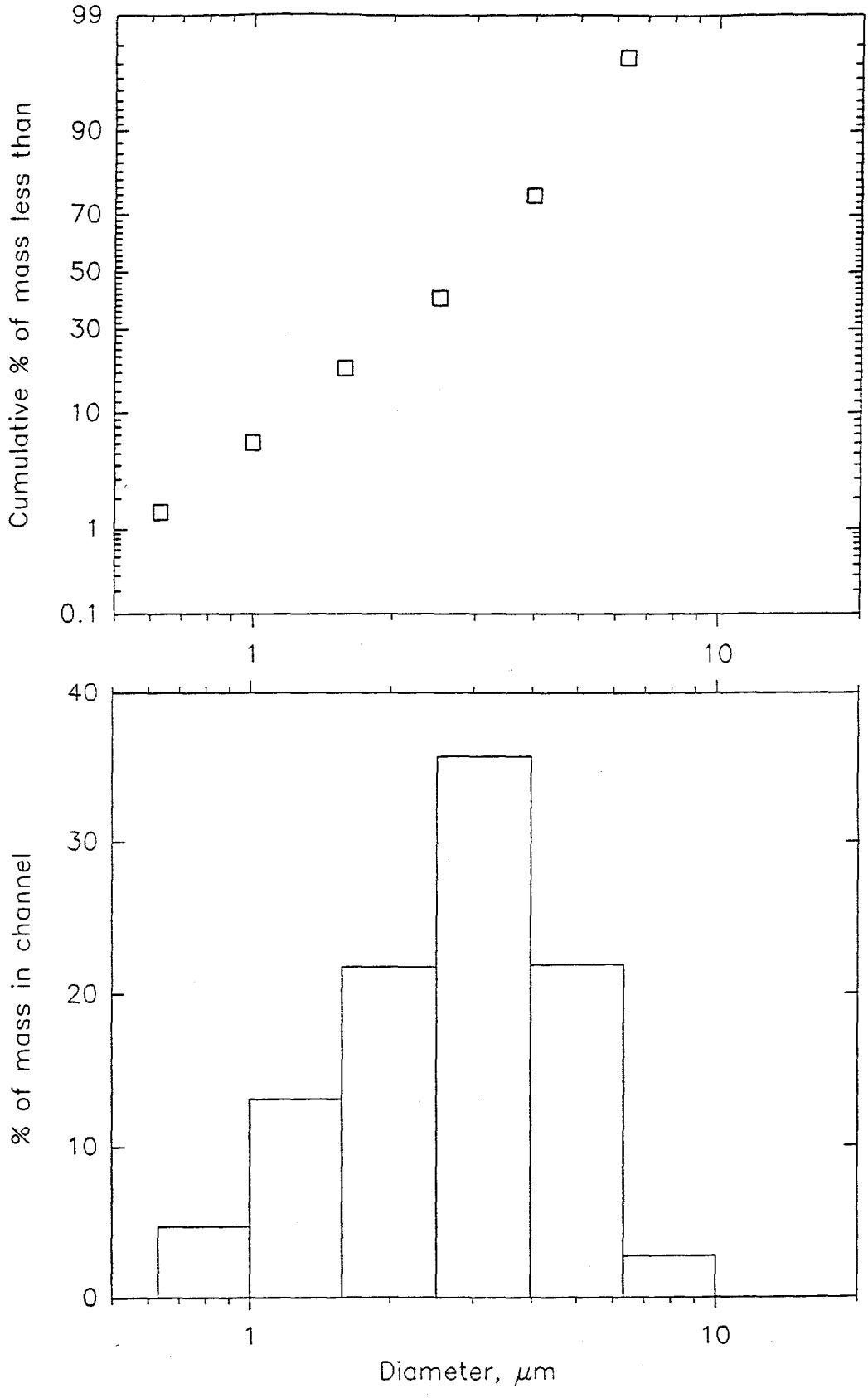

Figure 5. Cumulative and differential size distribution data measured with the sedigraph for ID # 4097 (TP, AS). The MMD of this ash is 2.8 μm.

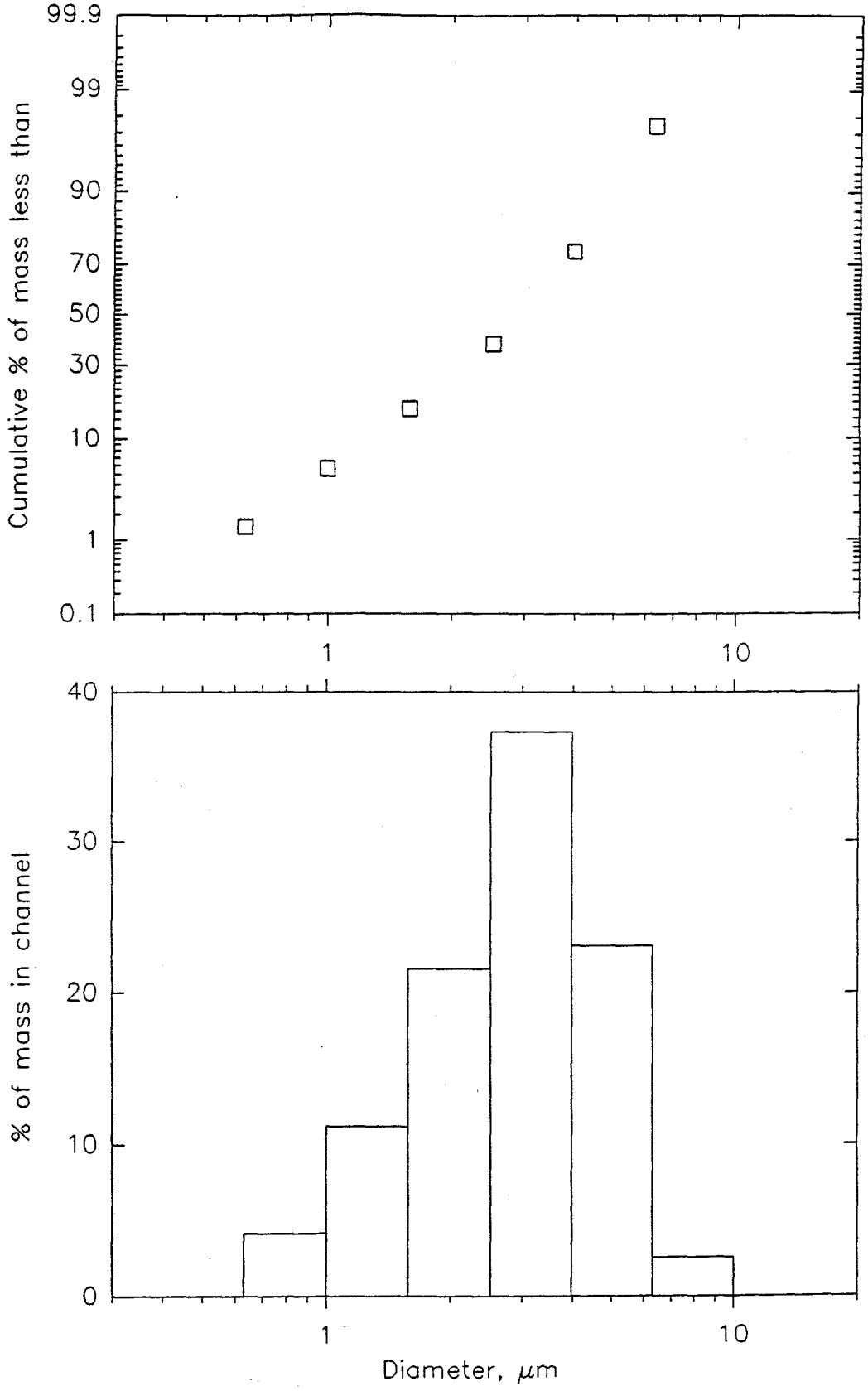

Figure 6. Cumulative and differential size distribution data measured with the sedigraph for ID # 4103 (BP, FC). The MMD of this ash is 2.9 μm.

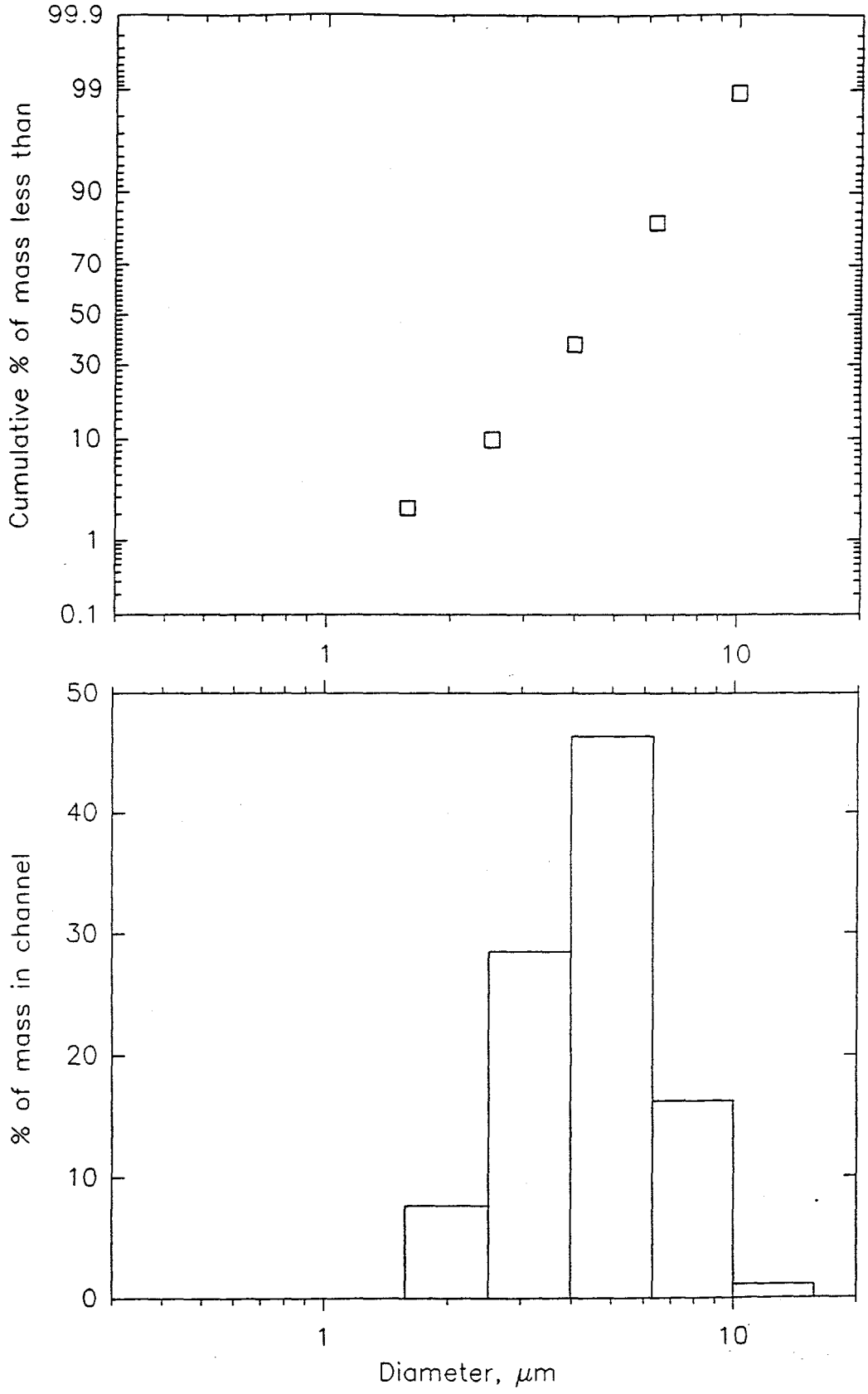

Figure 7. Cumulative and differential size distribution data measured with the sedigraph for ID # 4109 (MP, inside candle). The MMD of this ash is 4.5 μm.

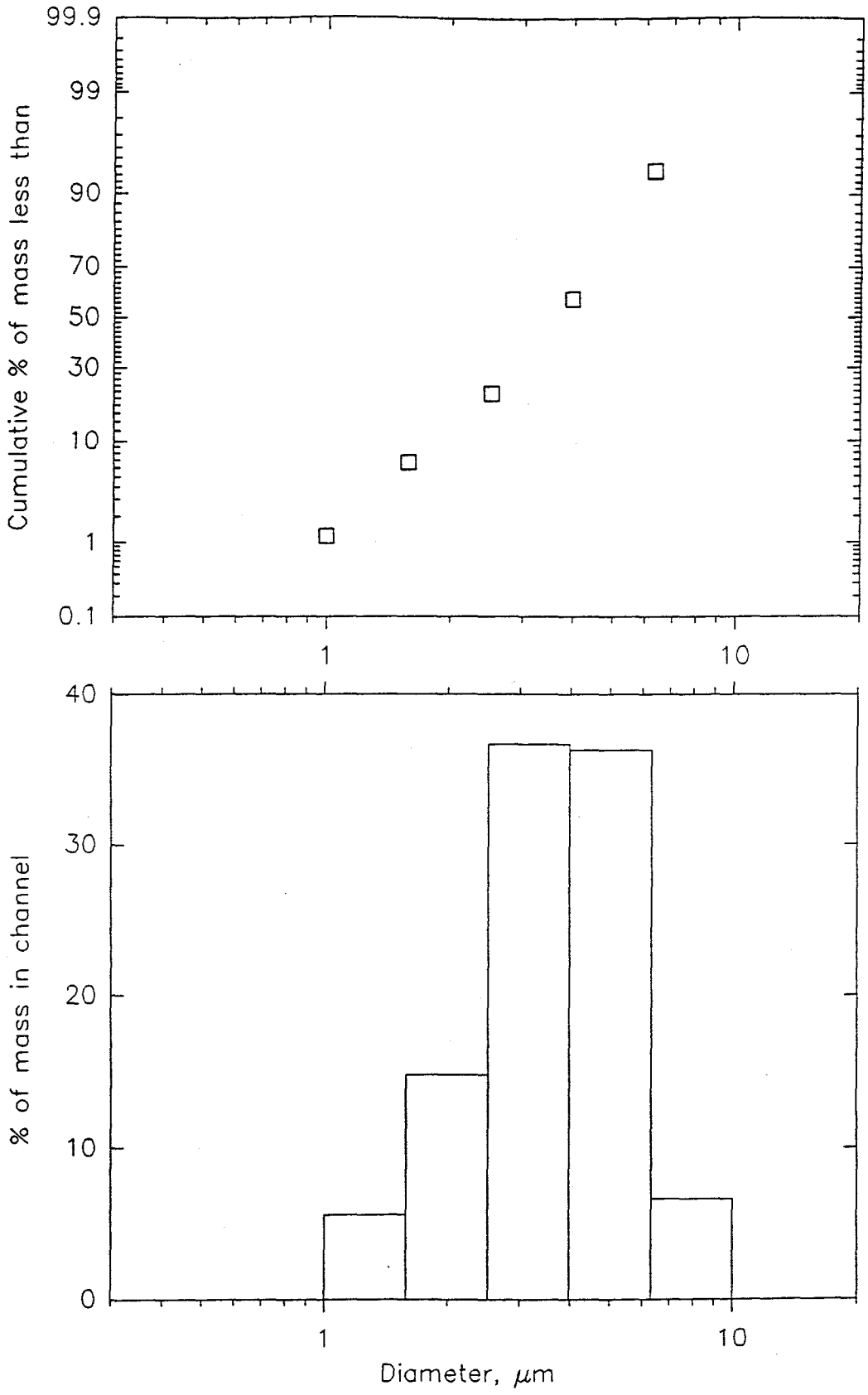

Figure 8. Cumulative and differential size distribution data measured with the sedigraph for ID # 4111 (MP, FC). The MMD of this ash is 3.6 μm.

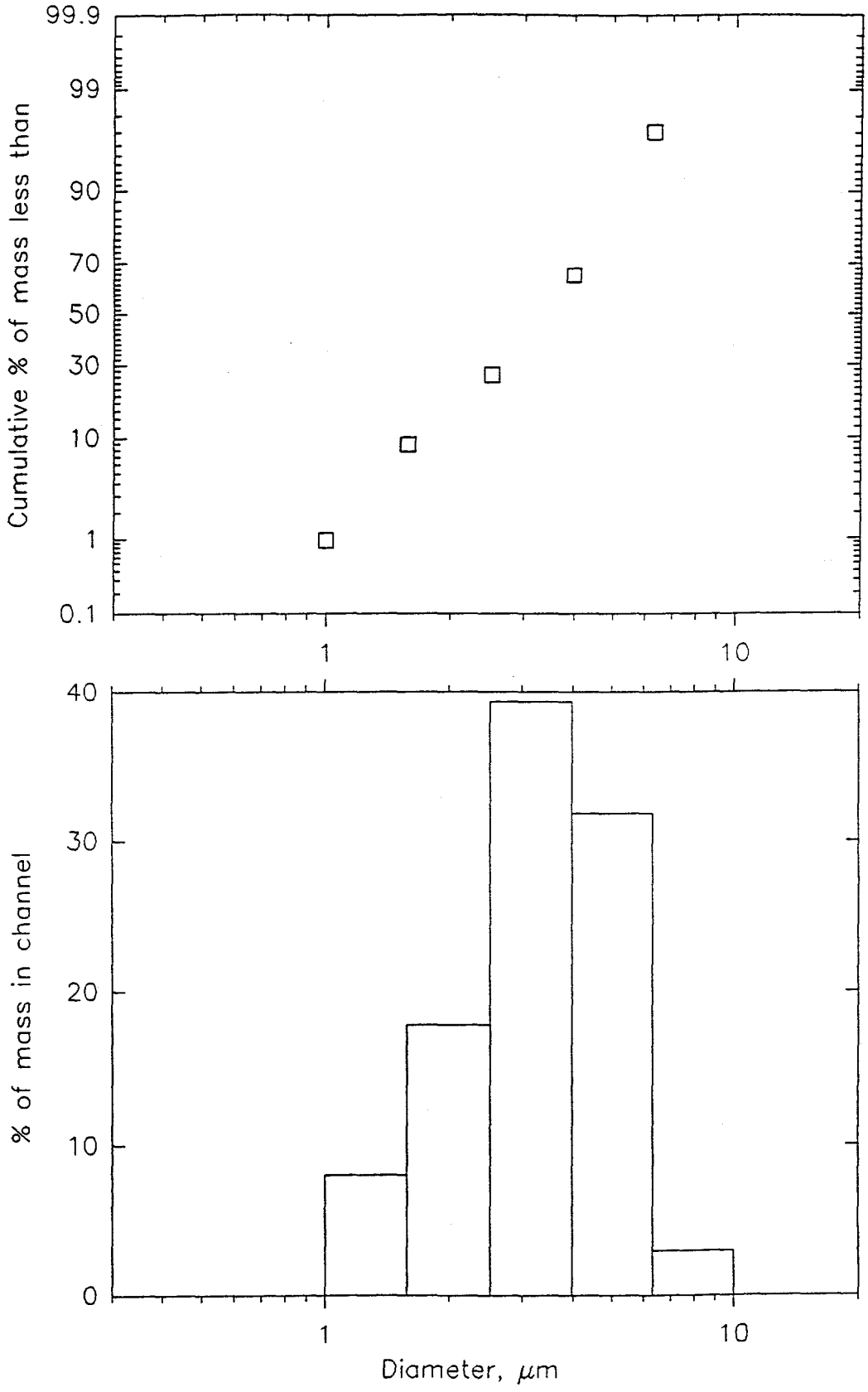

Figure 9. Cumulative and differential size distribution data measured with the sedigraph for ID # 4114 (MP, AS). The MMD of this ash is 3.3 μm.

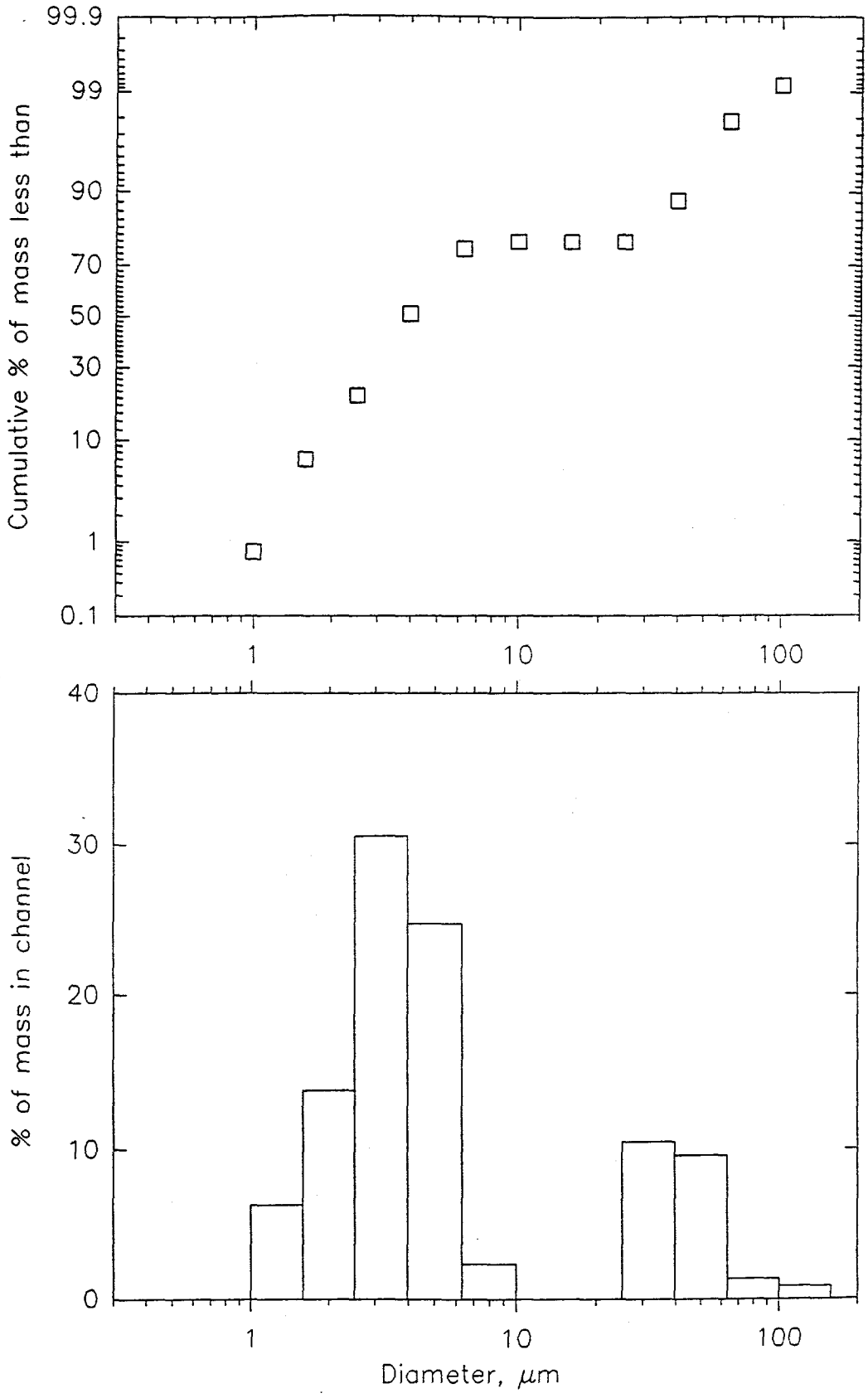

Figure 10. Cumulative and differential size distribution data measured with the sedigraph for ID # 4114 (MP, AS). The MMD of this ash is 3.9 μm, the D_{16} of this mass distribution = 2.1 μm, and the D_{84} of this mass distribution = 33 μm.

Table 3
Sedigraphic Size Distribution Data Measured for Ashes Collected at Tidd
fine portion only (< 20 μm)

ID #, location	Stokes' MMD, μm
2998, MP, AS	2.0
4079, MP, FC	2.4
4084, TP, AS	3.8
4097, BP, TS	2.8
4103, BP, FC	2.9
4109, MP	4.5
4111, MP, FC	3.6
4114, MP, AS	3.3
*4114, MP, AS	3.9

* complete size distribution

We also performed sieve analyses on two of the samples to verify the data we measured in the sedigraphic analyses. The results of these sieve analyses are included in Table 4. Because earlier studies have shown that at least 30 % by weight of the ash from Tidd is soluble in water, isopropyl alcohol was used to wash the ash through screens with 45 and 15 μm openings.

Table 4
Results of Sieve Analyses

	% by weight		
ID #, location	diam > 45 μm	45 μm > diam > 15 μm	diam < 15 μm
4097, BP, TS	4.03	17.34	78.63
4114, MP, AS	0.64	3.84	95.52

The particles too large to pass through the 45 μm sieve are different in appearance than the finer particles. Whereas the finer particles all seem to have the characteristic reddish-orange color associated with PFBC ashes, most of the larger particles are brown. A few of the larger particles are black or white.

It is evident for sample ID # 4114 (MP, AS) that the size distribution data for particle sizes greater than 20 μm measured with the sedigraph (approximately 22 % of the mass in particles greater than 20 μm diameter) differ from data obtained with the sieving technique (less than 5 % of the mass contained in particles greater than 15 μm diameter). Because of the problems the sedigraph has with samples having insufficient numbers of relatively large

particles, we believe the sieving data provide a more accurate measurement of the proportion of large particles. We are continuing these sieve analyses, and we may expand them to pass the fine fraction of the ash through 10 and 5 μm sieves, which we have available in our laboratory.

One of the purposes of performing sieve analyses was to compare the population of large particles in the ash deposits found on the top of the ash shedding cone under the middle plenum with the deposit that formed under the tube sheet at the top of the bottom plenum. These two sample locations are physically close to one another. These measurements were intended to determine if gravitational settling is the primary mechanism responsible for the presence of large particles in the ash deposits found at various locations in the filter vessel. If this were the case, we would expect that the sample taken from the ash shedding cone should have a significantly greater proportion of large particles than the sample from under the tube sheet. However, the data in Table 4 do not confirm this hypothesis. Since there is no active mechanism such as gas flow through the filter cake to carry particles to the region under the tube sheet, the whole size range of particles found in the deposits from this location must have been transported to the deposit by eddy diffusion and/or Brownian movement. In fact, the data in Table 4 show that particles comprising the ash deposit formed on the ash shedding cone are significantly finer than those from the deposit underneath the tube sheet. We have no explanation for this difference, and we will perform additional measurements to verify these results.

Scanning Electron Microscopy

We have performed a variety of Scanning Electron Microscopy (SEM) analyses on nodules and loose ash from sample ID # 4114 (MP, AS). The most crucial objective of these analyses was the determination of the composition of the interparticle bonds in the ash deposits formed in the filtration assembly. However, because the primary particles are relatively small (around 2 μm for the majority of particles), SEM EDX spectra and elemental maps do not have sufficient resolution to focus exclusively on the region of the interparticle bonds.

Figure 11 shows representative SEM photographs of loose ash particles from sample ID # 4114 (MP, AS). As suggested by our sieve analyses, these pictures indicate that particles larger than 10 μm diameter are the exception in this sample. The irregular shapes of the PFBC ash particles are apparent in these photographs. Figure 12 shows two views of an ash nodule that we have been examining with EDX spectra and elemental maps. So far these analyses have been inconclusive because of the resolution of the technique. The photographs illustrate the attachment of relatively small particles to larger structures within the nodule. It is not clear from these photographs if these larger structures are directly

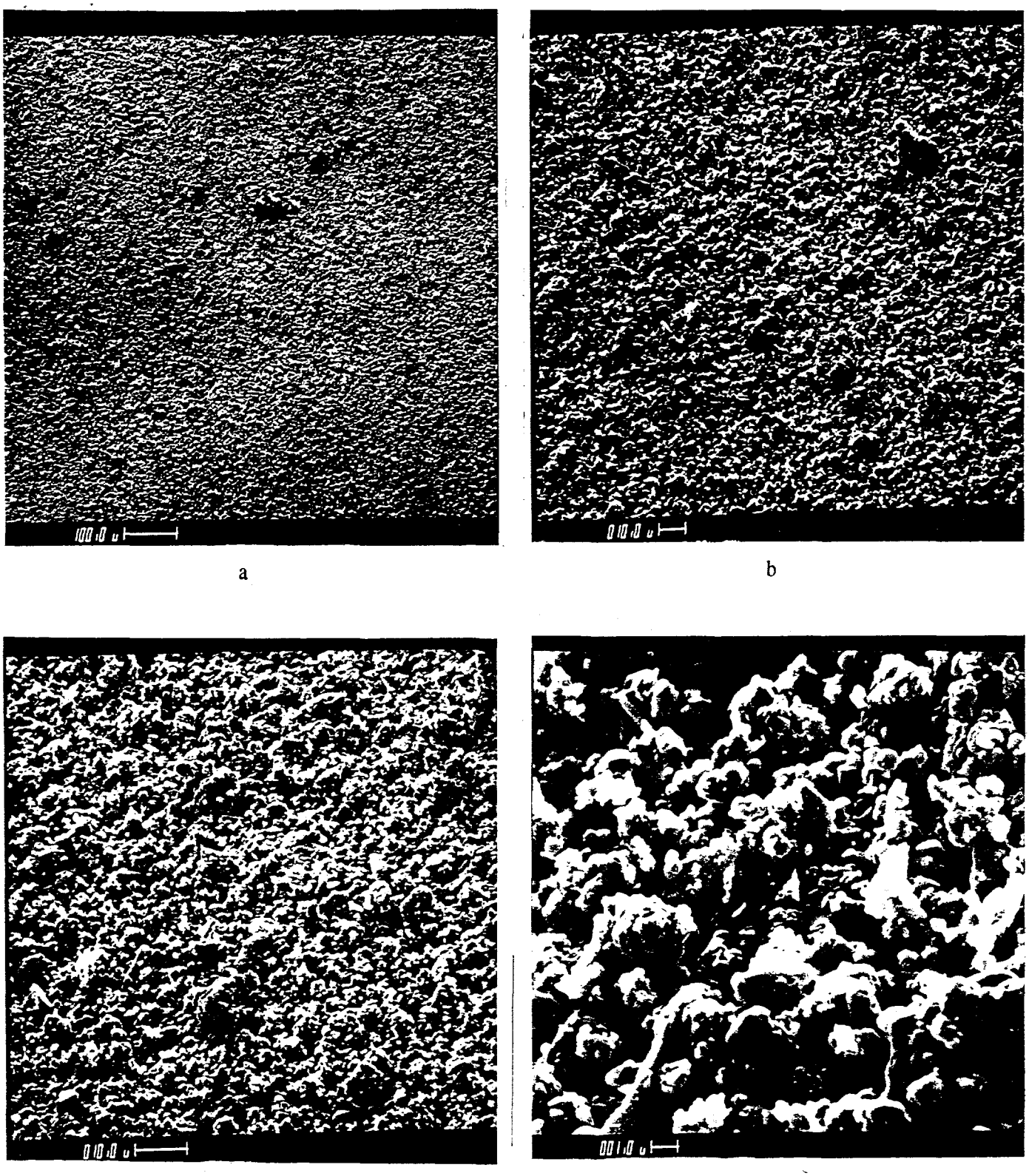

a b c d

Figure 11. Representative SEM photographs of ID # 4114 (MP, AS) ash taken at a) 100X, b) 500X, c) 1000X, and d) 5000X.

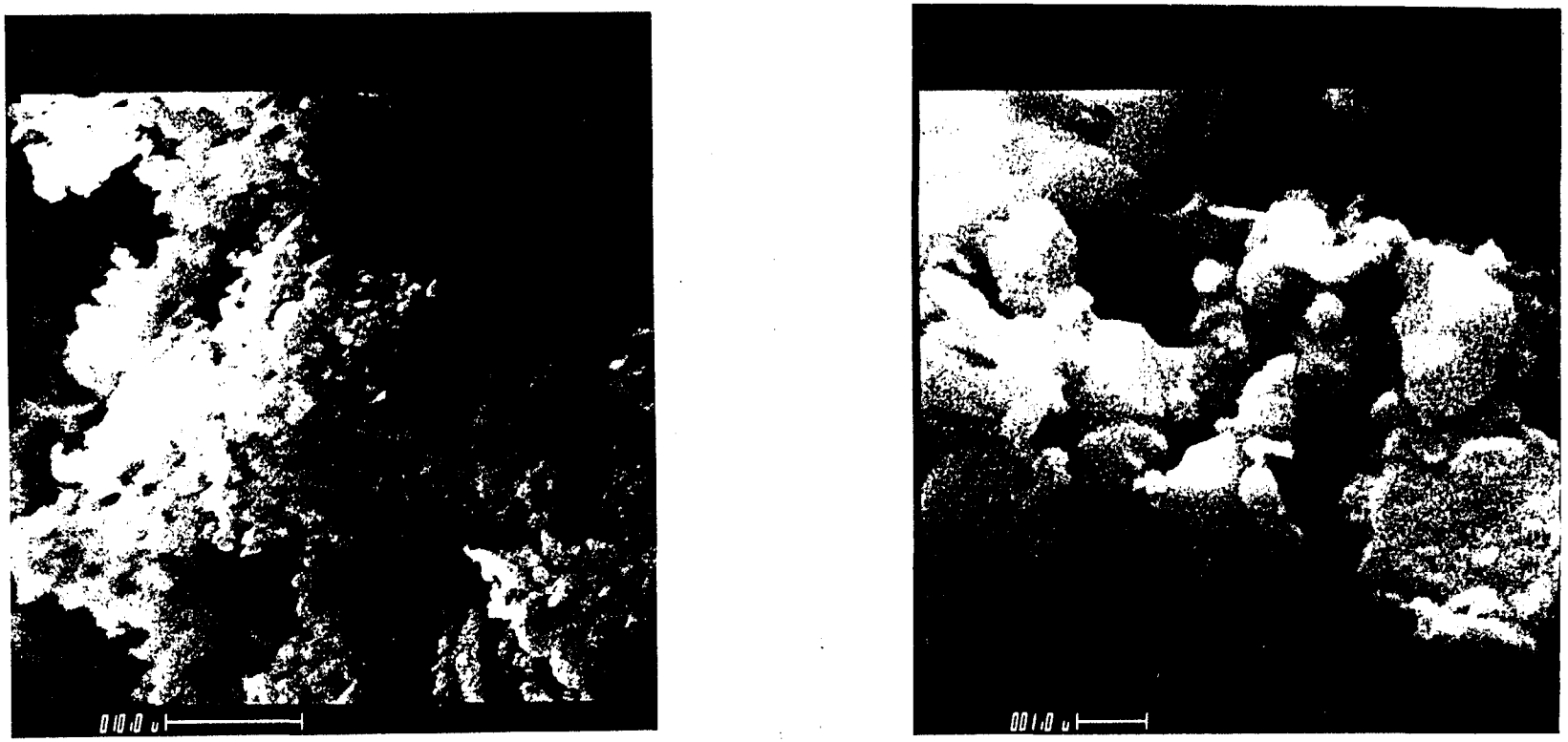

a b

Figure 12. Two representative SEM photographs of an ash nodule from sample ID # 4114 (MP, AS) ash taken at a) 2000X and b) 10,000X. The primary particles that make up the agglomerate seem to be strongly bonded together.

derived from relatively large particles or if these large structures are formed after particles are initially collected.

We also produced a pair of stereographic SEM photographs of a fresh fracture surface of a nodule taken from ID # 4114 (MP, AS). The stereographic image was very enlightening as to the structure of the nodule. However, because a special apparatus is required to obtain a true stereographic image from the SEM photographs we produced, only one of the two images is reproduced in Figure 13. The nodule appears to be a concretion composed of discrete fine particles almost completely embedded in a pervasive amorphous mass. Since the large mass in which the particles are embedded is almost certainly too large to have been formed during combustion and transported intact to the APF, it must have formed within the APF.

Based on the analyses we have completed, we are not certain of the origin of this amorphous mass. It may be composed of particles surrounded by some compound(s) that have condensed out of the flue gas. Another possibility is that unreacted calcium and/or magnesium present in the sorbent particles reacts with SO_2 in the flue gas to form calcium and/or magnesium sulfates. Since these alkali-sulfate salt molecules are physically larger than the original alkali molecules, the formation of these salts after the ash particles have been collected may result in lowered porosity, increased aggregate strength, and possibly the formation the type of concretion mentioned above. A third possibility is that eutectic mixtures are formed.

Studies of the buildup of boiler tube deposits in conventional pulverized-coal fired boilers describe the formation of eutectic mixtures which may lead to softening of the particles in the deposit and consequently account for the presence of an amorphous mass. Many of the ash particles collected in HGCU filter assemblies are derived directly from coal particles. These ash particles often contain a large percentage of aluminosilicate compounds. The other main source of ash particles is the sorbent used in the PFBC process. Sorbent-derived ash particles contain relatively large amounts of magnesium and/or calcium. Once these two types of ash particles come in contact with each other in the agglomerates formed in the filter vessel, the aluminosilicate compounds in the coal fly ash tend to react with alkali and alkaline metals in the sorbent ash particles to form eutectics that melt at relatively low temperatures. The progress of these reactions is supported by the intimate contact of the ash particles in the agglomerate and by long-term exposure of the ash particles to the temperatures in the filter vessel. As these eutectic mixtures melt, they might coalesce into the amorphous mass we observed.

Nodule Porosities

We encapsulated two nodules from sample ID # 4097 (BP, TS) on October 27, 1994 before leaving the Tidd Demonstration Plant. While on site, we also measured the

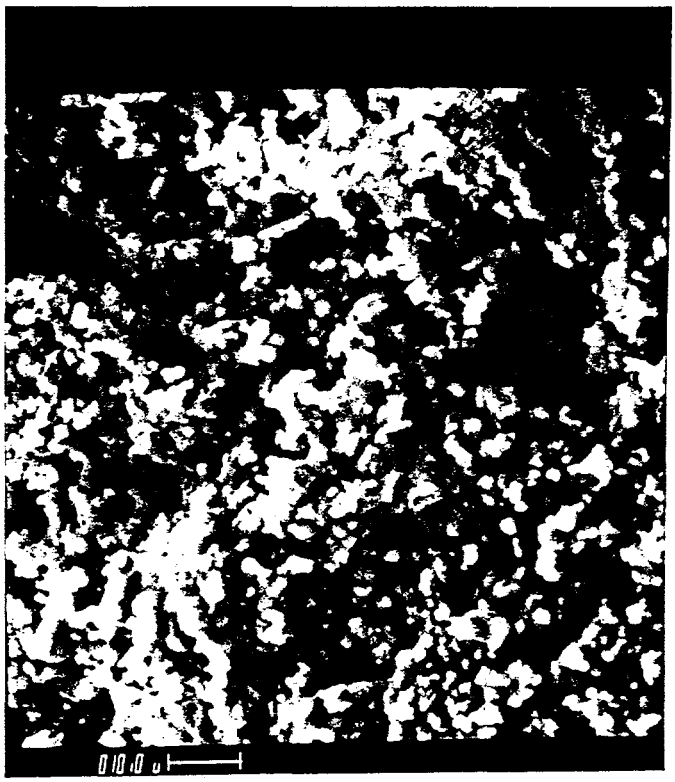

Figure 13. A representative SEM photograph of an ash nodule from sample ID # 4114 (MP, AS) taken at 1000X. The nodule appears to be an concretion composed of discrete fine particles almost completely embedded in a pervasive amorphous mass.

porosity of two nodules from sample ID # 4114 (MP, AS) and two more nodules from sample ID # 4116 (MP, AB) using the ethanol method described in Appendix A. These data are summarized in Table 5.

Table 5
Nodule Porosities Measured at Tidd

ID #, location	Porosity, % (epoxy encapsulation)	Porosity, % (ethanol method)
4097, BP, TS	85.8	--
4097, BP, TS	83.1	--
4114, MP, AS	--	83.7
4114, MP, AS	--	84.3
4116, MP, AB	--	82.5
4116, MP, AB	--	82.1

We also took a large nodule from sample ID # 4097 (BP, AS) and broke it into three pieces. The porosity of the first fraction was measured with the ethanol method. The second piece was baked at 1550 °F for 3 hours. The third piece was baked at 1550 °F for three days. The porosities of the two baked nodules were also measured with the ethanol method. These data are summarized in Table 6.

Table 6
Effects of Baking Duration at 1550 °F on the Porosity of # 4097 Nodule (BP, TS)

Duration, hr	Porosity, %
0	81.4
3	83.6
72	86.3

At present we are not certain what caused this apparent increase in porosity while the samples were being baked. Possibly the absorption and/or loss of water may account for these differences. Loose, sifted ash placed in the oven with these nodules consolidated slightly after 72 hours at 1550 °F during this trial. We plan additional baking tests to further investigate these effects.

We measured the uncompacted bulk porosities of loose sifted ash taken from ID # 4097 (BP, TS) and ID # 4114 (MP, AS). ID # 4097 (BP, TS) had an uncompacted porosity of 90.8 %, and ID # 4114 (MP, AS) had an uncompacted bulk porosity of 92.1 %. These

values are similar to those we have measured for Tidd ashes from earlier periods of operation.

FUTURE WORK

Additional sieve analyses will be conducted to further quantify the degree to which large particles become included in the various ash deposits formed in the APF. We also plan to compare the soluble sulfate levels in APF hopper ash and filter cake ash to determine if the concretion formed in the ash deposit is composed primarily of sulfate salts. We will also perform more baking tests to determine the effects of time and temperature on the porosity and mechanical strength of ash nodules and uncompacted samples of loose, sifted ash.

In addition to these analytical procedures, we will also begin to establish the structure of the interactive data base called for in the Task Plan.

APPENDIX A

NODULE POROSITY (WATER TECHNIQUE) - In this test, a nodule is selected, cleaned with a gentle jet of air, and weighed. Then water is allowed to soak very slowly into the nodule until the surface of the nodule glistens evenly. The fully wetted nodule is weighed, and the porosity of the nodule is calculated from the initial dry weight, the final wetted weight, and the true density of the ash particles. Determination of the porosity of a filter cake nodule provides a direct measurement of the porosity of the filter cake.

NODULE POROSITY (EPOXY TECHNIQUE) - In this test, a nodule is selected, cleaned with a gentle jet of air, and weighed. Then low-viscosity epoxy is allowed to soak slowly into the nodule until the surface of the nodule glistens evenly. The fully encapsulated nodule is baked to cure the epoxy, and its total volume is measured in a helium pycnometer. Nodule porosity is calculated from the initial dry weight, the final encapsulated volume, and the true density of the ash. Determination of the porosity of a filter cake nodule provides a direct measurement of the porosity of the filter cake. The cured, encapsulated nodule can be cut, machined, and prepared for further analyses, if desired.

STOKES' MASS MEAN DIAMETER - This technique uses a sedigraphic analyzer to provide a measurement of the fly ash size distribution based on aerodynamic classification of fly ash particles. The test procedure involves the suspension of a small amount of ash in a clear fluid. The particles in the fluid gradually settle out, first due to gravitational force alone, and then due to centrifugal force introduced by increasingly rapid rotation of the sample cell. The device combines photometrically-obtained particle concentration data with Stokes' law describing the settling of particles in a viscous medium to calculate the particle size distribution.

SPECIFIC SURFACE AREA - This measurement utilizes the Brunaeur-Emmett-Teller (BET) technique for determining the total surface area of a known mass of fly ash sample. Ashes that exhibit relatively high specific surface areas are usually highly cohesive, and form filter cakes with relatively high porosities.

UNCOMPACTED BULK POROSITY - This value expresses the porosity of a container of sifted ash. Ashes exhibiting a relatively high uncompacted bulk porosity value are generally highly cohesive.

DENSITY - This standard measurement is obtained with a helium pycnometer. The value obtained with this technique is the true density, or specific gravity of the ash particles in the sample tested.

DRAG-EQUIVALENT DIAMETER - This quantity is not a measurement of physical size, but rather a fitted parameter ranking the characteristic specific gas-flow resistances of ashes at equal porosities. Increasing values of drag-equivalent diameter indicate a lower resistance to gas flow at a given porosity. Measurements of physical size generally correlate with this expression; however, the drag-equivalent diameter best expresses the fineness of an ash as it relates to its effect on specific gas-flow resistance. Ashes with smaller values of drag-equivalent diameter are generally more cohesive.

SPECIFIC GAS-FLOW RESISTANCE - This value is obtained by filtering air at a known flowrate through a simulated filter cake of known porosity in a laboratory test device while measuring the resistance to the air flow. When this measurement is made with the porosity of the simulated filter cake equal to the estimated characteristic filter cake porosity of the ash, the resistance is defined as the specific gas-flow resistance. This value is the resistance that this simulated filter cake (with an areal loading of 1.0 lb/ft^2) exhibits for an air flow of 1.0 $acfm/ft^2$.

TENSILE STRENGTH - This test measures the magnitude of the attractive forces between ash particles. An electrostatic tensiometer is used to apply a mechanical stress on a dust layer as an effect of an imposed electrostatic field. This electrostatic technique allows the measurement to be performed on uncompacted ash samples.